Available online at www.sciencedirect.com

ScienceDirect

Procedia Engineering 109 (2015) 171 – 180

Procedia Engineering

www.elsevier.com/locate/procedia

XXIII Italian Group of Fracture Meeting, IGFXXIII

Experimental determination of compressive residual strength of a carbon/epoxy laminate after a near-edge impact

M.P. Falaschetti[a]*, M. Scafè[b], E. Troiani[a], V. Agostinelli[a], S. Sangiorgi[b]

[a] *MaSTeR Lab, Department of Industrial Engineering, University of Bologna, via Fontanelle 40, 47121 Forlì (FC), Italy*
[b]*Faenza Research Laboratories of ENEA – Faenza Technical Unit for Materials Technologies (UTTMATF), via Ravegnana 186, 48018 Faenza (RA), Italy*

Abstract

In this work has been estimated the compressive residual strength and Young modulus of a Carbon/Epoxy laminate after a near-edge impact.
Near-edge impacts were performed with a Charpy pendulus, modified in order to obtain impact tests comparable with the ASTM D7136/D7136M-12; whereas compressive tests were performed using the Wyoming Combined Loading Compression (CLC) Test Method, described in ASTM D 6641/D 6641M-09.
The CLC Test fixture presents many advantages: the load applied to the specimen is combined (end-load combined with shear-load), high reproducibility and reliability of the results, the lightness of the fixture, possibility of use specimens without tabs.
Twenty-six cross-ply ([0°/90°]ns) coupons were tested in the compressive tests: 10 after a 3J impact (5 central impact and 5 near-edge impact), 10 after a 5J impact (5 central impact and 5 near-edge impact), 6 specimens without impacts.

Peer-review under responsibility of the Gruppo Italiano Frattura (IGF)

Keywords: Impact; CAI; CFRP; CLC

* *Corresponding author. Tel.: +39 0543 374 421*
E-mail address: mariapi.falaschetti2@unibo.it

Peer-review under responsibility of the Gruppo Italiano Frattura (IGF)
doi:10.1016/j.proeng.2015.06.229

Nomenclature

ASTM	American Society for Testing and Materials
CAI	Compression After Impact
CFRP	Carbon Fiber Reinforced Polymer
CLC	Combined Loading Compression
E	Energy
$E_{absorbed}$	Absorbed energy
E_{actual}	Actual energy
$E_{residual}$	Residual energy
m	Mass
g	Gravitational acceleration
l	Attachment length
α	Angle of declivity
σ	Compressive residual strength
σ_{max}	Maximum compressive residual strength
σ_{mean}	Mean compressive residual strength
Sd. Dev.	Standard deviation
CV	Coefficient of variation
L	Applied Load
L_{max}	Maximum applied load
A	Cross-sectional Area
ε_x	Longitudinal strains measured by strain-gauge n°x
E_{mean}	Maximum value of longitudinal Young Modulus
% DEV	Percentage variation of a mean value to a reference value

1. Introduction

In the last twenty years, the pursuit to produce lighter structures has led the aeronautical industry to an increased use of composite materials, mostly carbon fibre reinforced polymers (CFRP). The Airbus A350 XWB is built of 52% CFRP, including wing spars and fuselage components, while the Boeing 787 Dreamliner has a 50% of weight. Furthermore, the Airbus A380 is one of the first commercial airliner to have a central wing box made of CFRP, with a smoothly contoured wing cross section instead of the wings being partitioned span-wise into sections, optimising the aerodynamic efficiency.

To ensure the safety of these structures, it is imperative to understand their fatigue behaviour. The challenging requirements set on new full composite aeronautical structures are mostly related to the demonstration of damage tolerance capability of their primary structures, required by the airworthiness bodies. And while composite-made structures inherently demonstrate exceptional fatigue properties, when put in real life working conditions, a number of external factors can lead to impact damages thus reducing drastically their fatigue resistance due to fibre delamination, disbonding or breaking.

For composite structure, aeronautical legislations affirm that aircraft constructors have to apply a factor of safety higher than that used for metallic ones. This because composites does not satisfy crack-growth principle used for metallic structures; thus, legislations require that composite structures have to satisfy “no-growth” principle [1]. The fatigue tests and analyses need to show this concept, which requires no initiation of new damage and no growth of existing damages. Impact tests are carried out in order to establish the behaviour of a composite structure when subjected to these impact loads and to determine the severity of the impact, based on different impact positions and energies.

1.1. Impact damages

In real conditions, there are many factors that influenced composites' characteristics and these have to be taken into account in design to satisfy aeronautical legislations. These factors are: humidity, operating temperature, impacts. Obviously, the last one has more evident effects than the others.

Impact damages can be classified on the basis of their detectability on structures' surfaces.

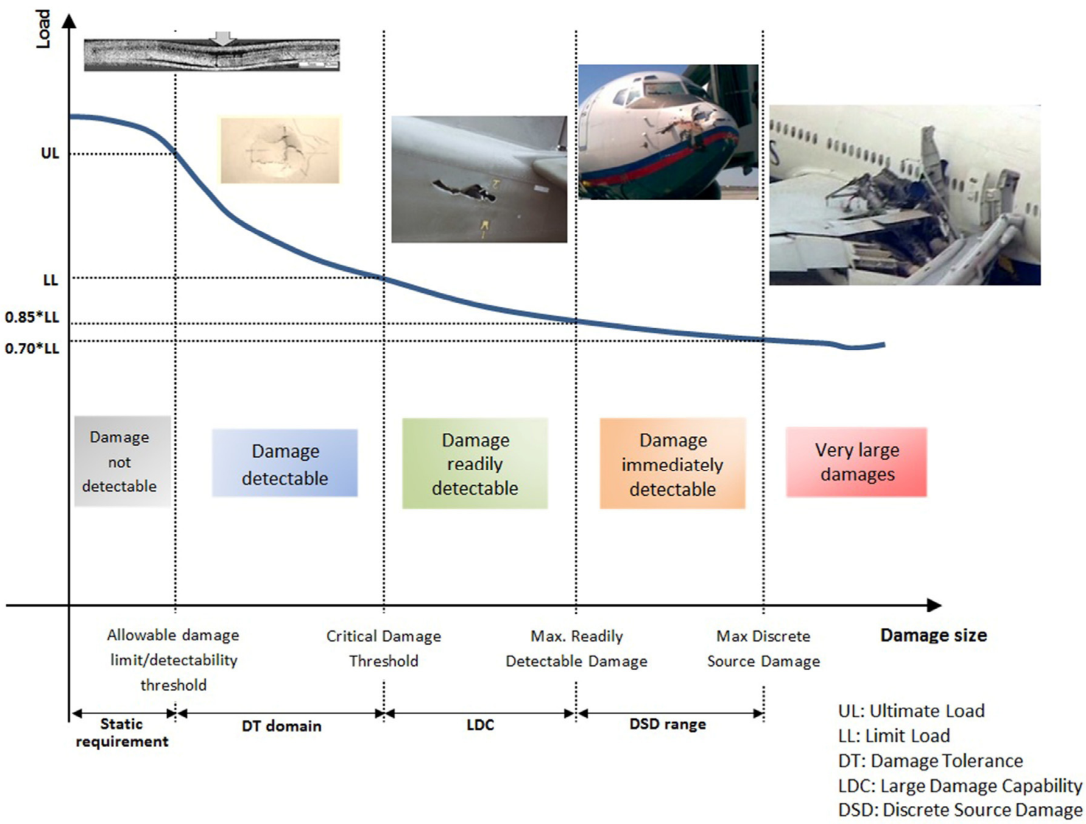

Figure 1. Damage size to load applied [2]

The most dangerous damages are certainly that commonly known as BVID (Barely Visible Impact Damages). They are not detectable with a simple visible inspection (without knowing the exact location of impact). Despite that, the resulting inner damage could be so widespread to cause a high reduction of structure mechanical characteristics.

This kind of damage could ensue from incidents during operative life or maintenance (e.g. little debris on the landing field crash into vehicle by wheels or high mass objects felt from little height like maintenance or assembly tools). [3]

In literature there are many studies about impacts according to ASTM D7136/D7136 M-12 [4] (central impacts on flat specimens). There are few, instead, studies about side impact (near-edge or on-edge impact) [5-7] inclusive of studies on glass fiber [8,9].

A side impact represent the worst condition because there is less material around the impact location contributing to the impact opposition. This kind of impact is the most probable event in a vehicle operating life bear in mind numerous cut-outs in the fuselage.

A not detectable impact damage through thickness of the structure could bring to sudden and catastrophic failure. Therefore, it is very important to understand impact influence on material characteristics.

Moreover damage size depends on many factors: impact energy, temperature, stacking sequence, laminate thickness, aging, etc [10]. Every one of them has to be analysed separately to evaluate their influence on material mechanical properties. In this paper is explained the experimental campaign done to understand influence of different impact energies on compression residual strength of a carbon/epoxy laminate.

2. Experimental

2.1. Specimens

Twenty-six specimens were cut from a 490x420mm laminate of carbon/epoxy composite [11].

Dimensions were according to compression test fixture used for CAI (Compression After Impact) [12] tests: it is the CLC (Combined Loading Compression) test fixture [13].

Length was chosen with reference to untabbed specimens (140mm); width was chosen as the allowable maximum value (30mm), compatible with CLC Test Fixture structural features. There is no limits for specimens thickness except for necessity of avoid coupons buckling. It was chosen a 9 plies stacking sequence ($[90/0_2/90/\overline{90}]_{2s}$) resulting in a mean coupons thickness of 2.6mm.

2.2. Impact tests

Specimens had been divided into 5 different groups every one characterized by 5 different kind of impact test (tab.1):

Table 1. Impact kind executed on specimen

Group	Impact kind	Energy
A	No impact	-
B	near-edge	3 J
C	near-edge	5 J
D	central	3 J
E	central	5 J

Impact tests were performed with a Charpy pendulum; it had been modified to obtain normal impact comparable with Drop weight test [4].

The swinging mass is a steel cylinder with a 7mm hemispherical impactor. Impact takes place when the mass attachment is perpendicular to ground surface meanwhile the impact direction is normal to the coupon surface.

During impact test, specimen is bonded in a specific fixture that allow to keep it in position and to settle impact location. For near-edge impact, a distance of 2.5mm from edge was chosen while for central tests hemispherical impactor has been settled to impact at the halfway width.

In both tests, impacts take place in middle of specimen length, in order to have the impact indentation in the centre of CLC gage section (untied section).

Every single impact was filmed with a camera to evaluate real release angle of the mass and the actual rebound angle. Therefore real impact energy and actual rebound energy were calculated thanks to (1):

$$E = mg\left(l - l\cos\alpha\right) \tag{1}$$

where E is energy, m impactator mass, g gravitational acceleration, l length of the mass attachment and α actual angle.

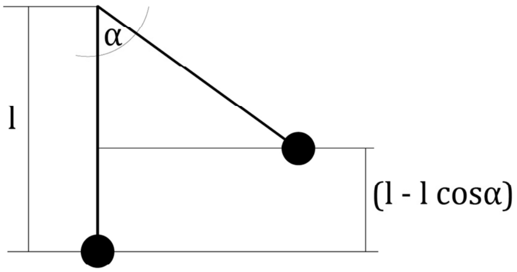

Figure 2. Schematised Charpy pendulus operation

Table 2. Energies of impacts

Specimen	Actual energy [J]	Residual energy [J]	Absorbed energy [J]
B1	3.342	0.907	2.435
B2	3.065	0.831	2.234
B3	3.065	1.244	1.821
B4	3.342	1.244	2.098
B5	3.202	1.336	1.866
C1	4.704	0.907	3.797
C2	4.866	1.244	3.622
C3	4.866	1.069	3.797
C4	4.704	0.986	3.724
C5	4.543	0.831	3.712
D1	3.342	1.155	2.187
D2	3.342	1.069	2.273
D3	3.484	1.069	2.415
D4	3.202	1.069	2.133
D5	3.202	0.986	2.216
E1	5.029	1.431	3.598
E2	5.196	1.529	3.667
E3	4.866	1.336	3.530
E4	4.543	1.244	3.299
E5	4.866	1.431	3.435

Due to these data, it was possible to calculate the energy absorbed by specimens (2):

$$E_{absorbed} = E_{actual} - E_{residual} \quad (2)$$

where $E_{absorbed}$ is the energy absorbed by material, E_{actual} is actual impact energy and $E_{residual}$ is impactator residual energy.

Hence every single test had been examined and data in Table 2 were obtained.

Therefore impacted specimens were visually inspected in order to pinpoint impacted location.

2.3. CAI tests

Compression After Impact (CAI) tests were performed with a CLC (Combined Loading Compression) Test Fixture as described in ASTM D6641/D6641 M-12 [13]. This test method presents some advantages compared to other composite materials compression test fixtures [14-16]:

- small and little complex test fixture simplifies tests (especially not room-temperature ones)
- combined load allows to test untabbed straight-sided specimens avoiding high stress concentrations;
- simple test method allows repeatable results.

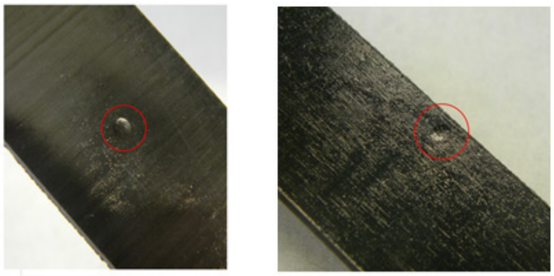

Figure 3. Examples of BVID due to a central impact (on the left) and a near edge impact (on the right)

The experimental tests were conducted at ambient laboratory conditions, using an MTS electro-hydraulic universal testing machine, equipped with an MTS 100 kN load cell. All tests were performed at a constant displacement rate of 1.3 mm/min, while the data were acquired at a rate of 10 samples/s and processed in accordance with the ASTM standard.

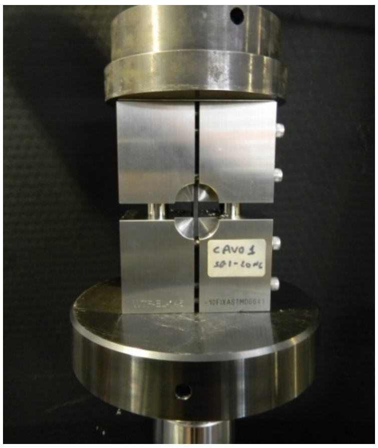

Figure 4. Specimen set in CLC test fixture on MTS machine

Every specimen residual compressive strength has been calculated with (3):

$$\sigma = \frac{L}{A} \tag{3}$$

where σ is residual compression strength, L is the maximum load applied, A is the cross-sectional area of the specimen. Results are summarized in Tab.3-7.

Table 3. Compressive test results of A samples.

Specimens	Cross-sectional area [mm^2]	Maximum load [N]	σ_{max} [MPa]
A0	87.1	-33351	-383.0
A1	82.0	-34172	-416.6
A2	87.9	-32845	-373.5
A3	87.3	-34216	-391.9
A4	85.9	-32593	-379.6
A5	84.0	-31091	-370.1
		σ_{mean} [MPa]	-385.8
		Sd. Dev. [MPa]	16.9
		CV [%]	4.4

Table 4. Compressive test results of B samples

Specimens	Cross-sectional area [mm^2]	Maximum load [N]	σ_{max} [MPa]
B1	69.8	-23913	-342.8
B2	81.9	-20118	-245.7
B3	84.5	-29537	-349.5
B4	89.1	-38055	-427.0
B5	88.1	-30601	-347.3
		σ_{mean} [MPa]	-342.5
		Sd. Dev. [MPa]	64.4
		CV [%]	18.8

Table 5. Compressive test results of C samples

Specimens	Cross-sectional area [mm^2]	Maximum load [N]	σ_{max} [MPa]
C1	84.1	-20473	-243.4
C2	84.9	-20684	-243.5
C3	84.4	-29630	-351.2
C4	86.8	-26366	-303.8
C5	87.1	-16114	-184.9
		σ_{mean} [MPa]	-265.3
		Sd. Dev. [MPa]	63.8
		CV [%]	24.0

Table 6. Compressive test results of D samples

Specimens	Cross-sectional area [mm^2]	Maximum load [N]	σ_{max} [MPa]
D1	68.7	-21924	-319.3
D2	81.2	-30936	-381.2
D3	72.4	-22220	-306.8
D4	81.7	-30050	-368.0
D5	71.0	-25746	-362.6
		σ_{mean} [MPa]	-347.6
		Sd. Dev. [MPa]	32.5
		CV [%]	9.4

Only one not impacted specimen was instrumented with two longitudinal strain gauges in configuration back to back. A Wheatstone bridge system in half-bridge configuration, was used for strain measurements.

The strain gauge configuration allows the determination of sample bending during the test time, by means of the following factor:

$$\text{Bending}[\%] = \frac{\varepsilon_1 - \varepsilon_2}{\varepsilon_1 + \varepsilon_2} * 100 \quad (4)$$

where ε_1 and ε_2 are the longitudinal strains measured by the two strain gauges [12].

Table 7. Compressive test results of E samples

Specimens	Cross-sectional area [mm^2]	Maximum load [N]	σ_{max} [MPa]
E1	81.4	-26725	-328.2
E2	84.8	-24547	-289.6
E3	83.6	-31050	-371.0
E4	84.2	-35774	-424.7
E5	82.1	-19922	-242.6
		σ_{mean} [MPa]	-331.2
		Sd. Dev. [MPa]	70.6
		CV [%]	21.3

The percent bending, as calculated in eq. (4), provides a reasonable indication of Euler buckling [12]. Failure and midpoint bending are reported in Tab. 8, as requested by ASTM D 6641. The latter is determined at the midpoint of the strain range used for chord modulus calculations [12].

Table 8. Compressive test results of A0 sample.

L_{max} [N]	σ_{max} [MPa]	E_{mean} [GPa]	% Bending failure	% Bending 2000με
-33351	-382.97	57.4	2.9	1.7

In the following Fig. 5 and 6 are showed plots obtained from A0 sample compressive test. Fig. 6 shows that the % bending of the sample is limited up to failure. This means that specimen had not incurred in Euler buckling and the test was well conducted.

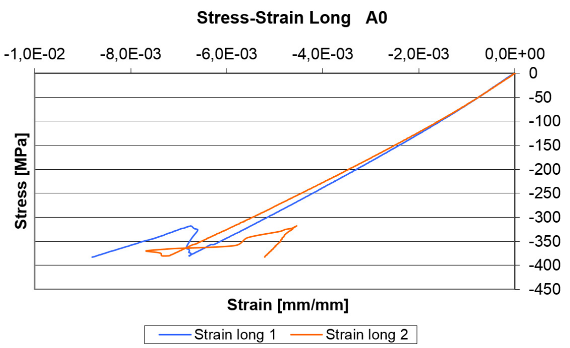

Figure 5. Stress-Strain curves of sample A0.

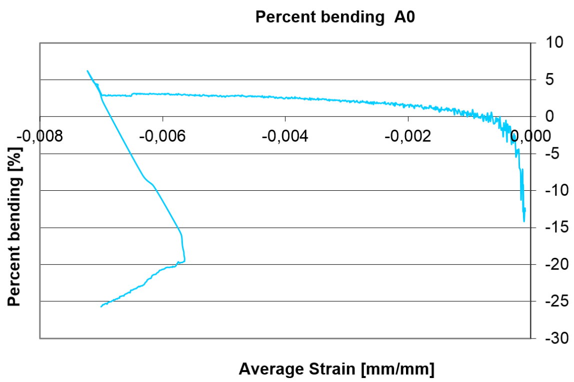

Figure 6. %Bending - Average Strain curve of sample A0

Mean values show a strong dependence of compressive residual strength to the kind of impact suffered. To make that more understandable, the percentage variation of compressive residual strength (compared with mean value of not impacted specimens $\sigma_{max} = -386.34\, MPa$) is summarized in Tab. 9.

Table 9. Results summary: mean compressive residual strength and % deviation to not impacted group

Group	σ_{mean} [MPa]	% DEV
B	-342.5	11.2
C	-265.4	31.2
D	-347.6	9.9
E	-331.2	14.1

It is possible to notice that all impacted specimens show a residual strength lower than that of pristine material. Especially 5J near-edge impacted specimens have a considerably lower compressive residual strength. Furthermore near-edge impacts are more influential on residual strength compared to central impact.

Therefore a 5J near-edge impact creates an inner damage that results in an extremely weakening configuration for compressive material characteristics. While a 3J energy impact modifies material characteristics irrespective of location (whether near-edge or not).

3. Conclusions

In the present paper the influence of different impact energies on compressive residual strength of carbon/epoxy laminate was examined.

Impact tests were performed with a modified Charpy pendulum in four different conditions. Then CAI tests were conducted with a CLC Test fixture. Six pristine specimens were tested with CLC test fixture as well; their compressive residual strength was taken as baseline to compare other results.

It was noticed that a low energy impact can result in a weakening inner damage even if impact location is hardly detectable (BVID). In particular, 3J energy showed an influence on compressive residual strength independent from impact location (near-edge or central), while 5J energy revealed to be a threshold value: a 5J near-edge impacted specimen has a reduction of compressive residual strength equal to double of that of one impacted centrally at the same energy.

Ultimately it was demonstrated the importance of understanding composites' behaviour after a low energy impact.

Acknowledgements

Special thanks go to Faenza Research Laboratories of ENEA – Faenza Technical Unit for Materials Technologies (UTTMATF), University of Bologna 'School of Engineering and architecture'.

References

[1] MIL-HDBK-17-1F – Composite Materials Handbook, Volume 1, Polymer Matrix Composites Guidelines for Characterization of Structural Materials, (2002).
[2] M. Calomfirescu, H. Hickethier, Damage tolerance of composite structures in aircraft industry, EADS Defence and Security, 2010.
[3] Serge Abrate, Impact on composite structure, Cambridge University Press, 2005.
[4] ASTM D7136/D7136 M-12 - Standard Test Method for Measuring the Damage Resistance of a Fiber-Reinforced Polymer Matrix Composite to a Drop-Weight Impact Event, 2012.

[5] C. Breen, F. Guild, M. Pavier, Impact Damage to Thick Carbon Reinforced Plastic Composite Laminates, J. Mater. Sci. 41 (2006) 6718-6724.

[6] A.T. Rhead, D. Marchant, R.Butler, Compressive Strength of Composite Laminates following Free Edge Impact, Composite Part A. 41 (2010) 1056-1065.

[7] N. Uda, K. Ono, K.Kunoo, Compression Fatigue Failure of CFRP Laminates with Impact Damage, Composite Science and Technology. 69 (2009) 2308-2314.

[8] A. Malhotra, F.J. Guild, M.J. Pavier, Edge Impact to Composite Laminates: Experiments and Simulations, J. Mater. Sci. 43 (2008) 6661-6667.

[9] A. Malhotra, F.J. Guild, Impact Damage to Composite Laminates: Effect of Impact Location, 2014.

[10] D. Ghelli, V. Cantarini, E. Troiani, Influence of Thermal cycling on the low velocity impact response of CRFP laminates, ECCM 16, European Conference on Composite Materials, Seville, Spain (2014)

[11] ASTM D 5687/D 5687 M-95 – Standard Guide for Preparation of Flat Composite Panels with Processing Guidelines for Specimen Preparation, (Reapproved 2007).

[12] ASTM D7137/D7137 M-12 - Standard Test Method for Compressive Residual Strength Properties of Damaged Polymer Matrix Composite Plates.

[13] ASTM D6641/D6641 M-14 - Standard Test Method for Compressive Properties of Polymer Matrix Composite Materials Using a Combined Loading Compression (CLC) Test Fixture, 2014.

[14] P.M. Wegner, D.F. Adams, Verification of the Combined Load Compression (CLC) Test Method, DOT/FAA/AR-00/26, 2000.

[15] M.Scafè, M.Labanti, A.Coglitore, G.Raiteri, R.Dlacic, E.Troiani, E.Besseghini, M.P.Falaschetti, Experimental determination of compressive strength of an unidirectional composite lamina: indirect estimate by Using Back-out Factor (BF), IGF, 2013.

[16] M.Scafè, G.Raiteri, A.Brentari, R.Dlacic, E.Troiani, M.P.Falaschetti, E.Besseghini, Estimate of compressive strength of an unidirectional composite lamina using cross-ply and angle-ply laminates, Frattura ed Integrità Strutturale, 29 (2014) 399-409; DOI: 10.3221/IGF-ESIS.29.35..